Self-Assembly and Its Impact on Interfacial Charge Transfer in Carbon Nanotube/P3HT Solar Cells

Marco Bernardi,[†] Michele Giulianini,[‡] and Jeffrey C. Grossman[†,*]

[†]Department of Materials Science and Engineering, Massachusetts Institute of Technology, 77 Massachusetts Avenue, Cambridge, Massachusetts 02139-4307, United States, and [‡]School of Engineering Systems, Queensland University of Technology, 2 George Street, Brisbane, Queensland 4001, Australia

ABSTRACT Charge transfer at the interface of conjugated polymer and nanoscale inorganic acceptors is pivotal in determining the efficiency of excitonic solar cells. Despite intense efforts, carbon nanotube/polymer solar cells have resulted in disappointing efficiencies (<2%) due in large part to poor charge transfer at the interface. While the interfacial energy level alignment is clearly important, the self-assembly and the interface structure also play a major role in facilitating this charge transfer. To understand and control this effect to our advantage, we study the interface of commonly used conductive polymer poly-3-hexylthiophene (P3HT) and single-walled carbon nanotubes (SWNTs) with a combination of molecular dynamics simulations, absorption spectra experiments, and an analysis of charge transfer effects. Classical molecular dynamics simulations show that the P3HT wraps around the SWNTs in a number of different conformations, including helices, bundles, and more elongated conformations that maximize planar $\pi-\pi$ stacking, in agreement with recent experimental observations. Snapshots from the MD simulations reveal that the carbon nanotubes play an important templating role of increasing the π-conjugation in the system, an effect deriving from the $\pi-\pi$ stacking interaction at the interface and the 1-dimensional (1D) nature of the SWNTs, and independent of the SWNT chirality. We show how this increase in the system conjugation could largely improve the charge transfer in P3HT—SWNT type II heterojunctions and support our results with absorption spectra measurements of mixtures of carbon nanotubes and P3HT. These findings open possibilities for improved preparation of polymeric solar cells based on carbon nanotubes and on 1D nanomaterials in general.

KEYWORDS: self-assembly · organic photovoltaics · excitonic solar cells · bulk heterojunction · P3HT · conjugation length · carbon nanotube · molecular dynamics · charge transfer

Mixtures of carbon nanomaterials and conjugated polymers have been used extensively as active materials in excitonic solar cells[1] (XSC). Poly-3-hexylthiophene (P3HT) has proven thus far to be one of the best choices for the donor material in bulk heterojunction XSC,[2] and its use in conjunction with single-walled carbon nanotubes (SWNTs)[3−7] as the acceptor material is considered a natural combination due to the very good hole and electron mobilities in the two materials, respectively, and the potentially ideal morphology of their distributed heterojunction—provided effective phase separation—at the nanoscale. Yet, despite this potential, P3HT−SWNT blends have shown limited performance under solar cell device operation,[5] with much lower efficiencies and photocurrents to date compared to the related [6,6]-phenyl-C_{61}-butyric acid methyl ester (PCBM)−P3HT solar cells.[8] While early experimental characterization of P3HT−SWNT blends provided important insight into their electrical, optical, and structural properties,[9,10] much of the physics and chemistry of nanostructured inorganic−organic heterojunctions used in XSC can only be understood by knowing their detailed interface and electronic structure at the molecular scale.[11,12] For example, an NMR study by Yang *et al.*[12] revealed the crucial role played by the nanoscale arrangement of P3HT at the interface with PCBM, where annealing induces local separation of P3HT sheets and enhances the charge transfer at the interface. This work suggests that two main factors contribute to the efficiency of charge transfer at the interface: the formation of a favorable type-II heterojunction in which the built-in field favors effective charge transfer (that is, the "electronic" factor), and the structure of the donor molecules at the interface, where extended polymer conjugation (like in the phase-separated polymer sheets shown in ref 12) favors charge transfer analogous to the effect of crystalline regions in the bulk of semiconducting polymers (*i.e.*, the "structural" factor).

Recent theoretical studies of idealized P3HT−SWNT interfaces[4] showed that only semiconducting SWNTs form favorable type-II heterojunctions with P3HT, while in the metallic SWNT case the P3HT transfers a significant amount of charge before equilibration and makes the nanotubes unlikely

*Address correspondence to jcg@mit.edu.

Received for review July 29, 2010 and accepted October 18, 2010.

Published online Xxxxxxxxx 00, 0000
10.1021/nn1018297

to act as electron acceptors in the device. Since in a SWNT sample of random chirality approximately one-third of the nanotubes are metallic,[13] the presence of these interfaces with a large build-up of static charge can undermine charge diffusion and transfer in the whole device. Improvements in SWNT sorting[14] make it now possible in principle to manufacture XSC made of blends of P3HT and only semiconducting SWNTs, though a similar device has not been shown yet.

In contrast to the electronic behavior at these junctions, we have a much less complete picture of the influence of the molecular organization on the charge transfer at this interface. Recent scanning tunneling microscopy[15] and high-resolution transmission electron microscopy measurements[16] of the interfacial structure of P3HT and SWNTs revealed polymer structures ranging from helical assemblies to more disordered, bundled conformations. These and other experiments[17] confirmed the picture that P3HT adsorbs strongly, beginning in solution, to the SWNTs through $\pi-\pi$ stacking forces. Theoretical work has thus far been limited to the consideration of ideal structural conformations, with the polymer placed either perpendicular or parallel to the SWNTs due to computational expense. Yet, a deeper understanding of the structure−property relationships and molecular scale self-assembly process for the P3HT−SWNT interface could lead to important insight regarding optimal regimes in which these nanotube-based XSC blends should be prepared, analogous to the case of PBCM. To this end, classical molecular dynamics (MD) simulations[18,19] can be used to provide important insights by allowing direct access to nanoscale self-assembly processes.[20]

In this work, a combined theoretical and experimental approach is employed to shed light on the structure−property relationships of P3HT−SWNT interfaces. MD simulations are performed to predict and understand the interfacial structure of P3HT with a number of SWNT chiralities and diameters. Since the π-conjugation of the polymer at the interface plays a crucial role in the charge transfer, we combine an analysis of the MD trajectories[21] with optical absorption measurements to provide an accurate picture of the nature of the self-assembly and its impact on the π-conjugation at the SWNT−P3HT interface. Systems with varying relative concentrations of P3HT and SWNTs are investigated and allow us to elucidate the self-assembly process in solutions of P3HT and SWNTs commonly used for spin-casting of thin film devices. Taken together, our results show that P3HT attains a higher conjugation with increasing SWNT content, and this in turn impacts the charge transfer at the interface significantly.

RESULTS AND DISCUSSION

Self-Assembly and Molecular Dynamics Simulation. We performed MD simulations using the LAMMPS MD code[22,23] at constant temperature (300 K unless otherwise stated) using the Nose−Hoover thermostat and a time step of 1 fs. In most simulations we used 20-repeat-units long regioregular P3HT (rr-P3HT 20-mer, *i.e.*, 40 thiophene rings), which corresponds to approximately 1/10 of the length of commercially available high purity rr-P3HT. The chains were initialized in the all-trans configuration and relaxed with the conjugate gradient method. A combination of classical force fields[24−30] was used to describe the intramolecular degrees of freedom of the P3HT and the SWNTs and their intermolecular interaction (see Methods).

In a first set of simulation runs, a single P3HT molecule was initialized at a distance of 9−10 Å from a single SWNT surface. The P3HT was prepared orthogonal or parallel to the SWNT axis, analogous to the configurations used in previous electronic structure calculations,[4] and relaxed before the simulation run. Since in the experiment P3HT encounters SWNTs with different structure, it is interesting to investigate the roles of the SWNT diameter and chirality in the self-assembly process. To this end, we used in the simulations zigzag (15,0), chiral (10,4), and armchair (8,8) SWNTs of similar diameter of approximately 12 Å, as well as SWNTs with diameters as small as 4 Å and as large as 40 Å. Both P3HT 20-mers and 50-mers (100 thiophene rings) were used in the simulations.

A typical run with orthogonal P3HT initialization proceeds as shown in Figure 1a. The P3HT molecule initially adsorbs and folds around the SWNT during the first 100 ps (equilibration part of the run), over which the energy decreases steadily (Figure 1d). After approximately 100 ps, the molecule is adsorbed at the SWNT surface, partially extends along the axis and continues folding around the nanotube to some extent, while the energy oscillates around a constant value. This indicates that the folding of P3HT on SWNT is a relatively fast phenomenon (100 ps) and following this the P3HT equilibrates and remains bound to the SWNT surface. A similar trajectory is observed regardless of the SWNT chirality and diameter for a P3HT 20-mer with orthogonal initialization. A close-up of a local helix formed at 70 ps during the folding (Figure 1b) shows a pitch distance of 5.1 Å for a (15,0) SWNT, consistent with the STM measured distance of 5.4 $\pm$ 0.7 Å for the same SWNT.[15] It is interesting to follow the distance between the two sulfur atoms S1 and S2 that form the pitch distance in the helical conformation of Figure 1b. Upon folding, these S atoms get closer (Figure 1c), and as the chain starts unfolding local minima in the distance as a function of time (for example, at 70 ps, where the snapshot at Figure 1b was extracted) occur and correspond to helical conformations. Equilibrium is attained after 100 ps following which this distance stabilizes to a value typical for the chain aligned along the nanotube with the presence of some local curves.

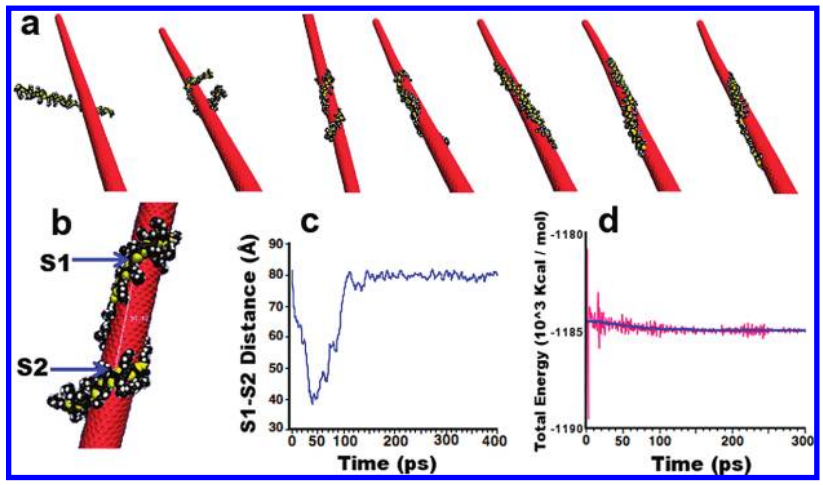

Figure 1. Simulation run of a P3HT 20-mer (40 thiophene rings) initialized orthogonal to a (15,0) SWNT. (a) Folding occurs in the first 100 ps (equilibration part of the run, snapshots 1−3) followed by evolution through a more elongated conformation during the production run. (See the Supporting Information for the full video.) (b) Detail of the helix observed at approximately 70 ps. The pitch distance is approximately 5.1 Å between the sulfur atoms S1 and S2 marked in Figure. (c) Time evolution of the distance between S1−S2, with a dip during the folding and a value that stabilizes following the equilibration. (d) The energy decreases steadily during the first 100 ps corresponding to the polymer adsorption and folding. The energy oscillates about a constant value following the equilibration.

All the runs with parallel initialization show similar results to the orthogonal case after equilibration, that is, the P3HT extends along the SWNT axis and makes partial curls, but no initial folding occurs upon adsorption. After equilibration, it is the competition between the $\pi-\pi$ stacking interaction and the torsional rigidity of the polymer that drives the chain dynamics. Cases in which the polymer chain is kinetically "stuck" (as opposed to in dynamic evolution) at the interface with the SWNT in more disordered conformations were also observed. For example, when a 50-mer is initialized orthogonal to a (15,0) SWNT, the folding becomes irreversible, and the P3HT is kinetically trapped (within MD time scale) in a "bundled" conformation that well resembles recent experimental observations.[16] A comparison of the helical and disordered (bundled) conformations is shown in Figure 2. Since most of the self-assembly begins already in the solution where P3HT and SWNTs are mixed prior to film deposition,[17] these results are representative of single bare-SWNT−P3HT encounters within the solution.[31]

We interpret these trends as a tendency of P3HT to fold around a SWNT when approaching it at a large local angle to the axis; in these circumstances, helices and more regular shapes may be kinetically stabilized and therefore observed using nanometer-resolved imaging tools.[15] The adoption of more disordered (Figure 2b) as well as more stretched P3HT conformations is also possible.

Unless a single junction device is desired between P3HT−SWNT, the assembly of a larger set of chains and SWNT is what occurs during a typical P3HT−SWNT film preparation. To explore this regime we performed larger scale MD simulations, where, in contrast to the simulations discussed so far, a large variety of initial P3HT conformations interacting with SWNTs are sampled in order to give a picture of the overall self-assembly process unbiased by the initial geometry. Twenty P3HT 20-mer chains were initialized in the all-trans conformation and at random locations in a cubic box of side 200 Å. Periodic boundary conditions (PBC) were imposed throughout the runs to resemble an infinite medium. The initial configuration had a density of *ca.* 1/40 that of bulk P3HT (1.1 g/cm^3), resembling the situation of a drying P3HT−SWNT solution where most of the solvent has been previously evaporated.[31] SWNTs of type (15,0) and length 5 and 15 nm were added to the P3HT to simulate blends with SWNTs weight fractions in the range of 0−40 wt %.

Figure 3 shows a simulation run where four SWNTs of length 15 nm (equivalent to approximately a SWNT weight fraction of 40%) were initialized in the simulation box together with the 20 P3HT 20-mer molecules.[32] Multiple P3HT molecules adsorb onto the SWNTs over the first 100 ps similar to what was observed above for the single P3HT−SWNT simulations. Small bunches of SWNTs form within 500 ps where each SWNT is coated

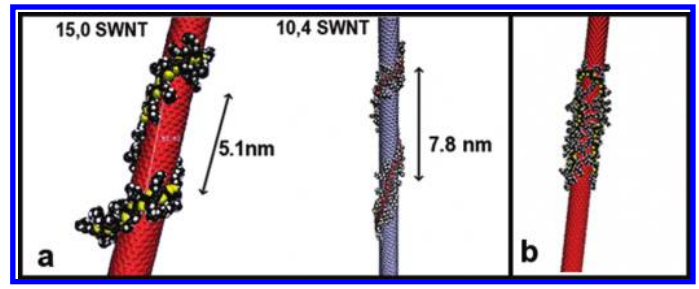

Figure 2. Locally stable conformations found during the simulation runs and also observed experimentally. (a) Helices form on (15,0) and (10,4) SWNTs during the folding of P3HT 20-mers with orthogonal initialization. The chirality may affect the pitch distance to some extent, but is not crucial in determining the overall time evolution or the simulation runs. (b) A P3HT 50-mer is kinetically trapped in a bundled, disordered shape that well matches recent experimental observations (ref 16).

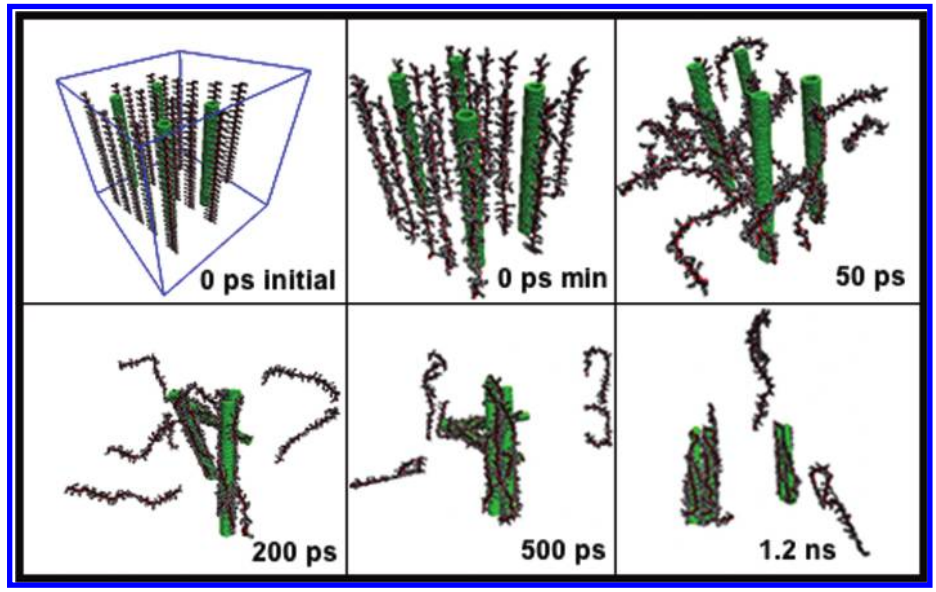

Figure 3. Simulation run of 20 P3HT 20-mer molecules and 40% wt (15,0) SWNT (30 000 atoms total) in a simulation box with periodic boundary conditions (here unwrapped after the run for ease of visualization). The P3HT molecules start adsorbing in the first 100 ps and complete the adsorption within 500 ps. Following this the SWNT and P3HT dynamics is strongly correlated as small bunches of SWNT form coated and intimately mixed with P3HT molecules. The chains that do not adsorb on the nanotube contribute to the formation of all-P3HT domains. (See the Supporting Information for the full video.)

by P3HT molecules. This effect is consistent with the experimental observation of the debundling effect played by P3HT, and is of great technological relevance.[17] Analogous effects are seen at smaller concentrations and for SWNTs of both lengths (see the Supporting Information for full videos).

Analysis of the Conjugation Length. In addition to the structural information regarding the assembly process discussed thus far, we can also gain information from the MD simulations regarding changes in the π-conjugation length at the interface due to the templating role of SWNTs upon P3HT adsorption. This effect is important for the resulting solar cell efficiency, as it could strongly impact the charge transfer at the interface, provided favorable electronic level alignment is present.

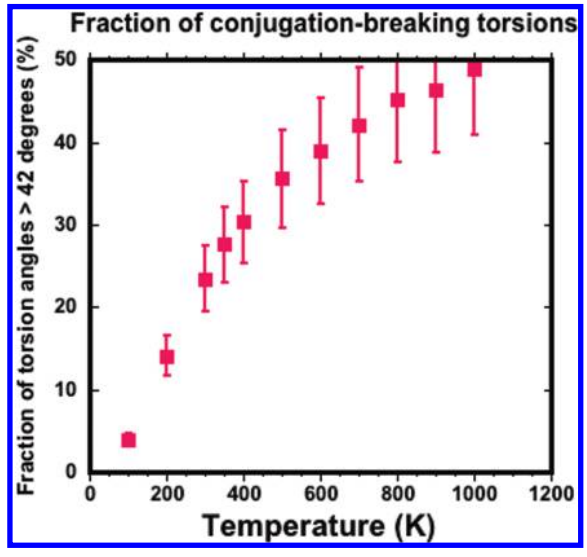

Figure 4. Fraction of conjugation-breaking angles as a function of temperature for a single P3HT 20-mer (see text for details).

The electronic wave functions in the conduction band and valence band of P3HT are localized over several thiophene rings of a single chain, mostly caused by ring−ring torsion angles in excess of approximately 40°.[21,33] From our MD simulations, we calculated the fraction *f* of "conjugation-breaking" torsion angles whose difference from 0° or 180° is larger than 40°[34] by obtaining the ring normal unit vectors and consequently the torsion angles between adjacent thiophene rings for a large number of different simulations. Comparing the value of *f* in the presence of the SWNTs with that found for pure P3HT at the same temperature of 300 K, we found a sizable decrease of *f* in all simulation runs where SWNTs were present. We note that *f* is inversely proportional to the conjugation length, since 1/*f* is the conjugation length in units of ring-to-ring distance. Therefore, a higher value of *f* corresponds to a smaller conjugation length, with inverse proportionality. We first used this method to analyze a single P3HT chain as a function of temperature (Figure 4). At low *T* a small value of *f* is expected since few rings will be able to overcome the intrinsic torsion barriers present in the P3HT molecules, while at large *T* the value of *f* should saturate to 96/180 ≈ 0.53 (or 53%), that is, the value for completely random torsion angles expected when k_BT is much larger than all torsion barriers. We found that *f* increases from approximately 4 ± 1% at 100 K to 49 ± 8% at 1000 K, consistent with a picture of a polymer with finite torsional rigidity, and a value of f_{300} = 23.5 ± 6.1% at room temperature (300 K).[35]

For comparison, the simulations with a single P3HT and a single SWNT discussed above were analyzed with

the same procedure. The values of f were found to be in the range 1−2% for parallel and orthogonal P3HT 20-mer initializations (due to the initial folding, this value would be $f \approx 4-5\%$ for the orthogonal case if the first 100 ps of equilibration were not discarded) and for a large number of nanotube chiralities. The maximum f value found in this set of runs is for the P3HT 50-mer with orthogonal initialization (Figure 2b) that assembled into a bundled (disordered) structure where a maximum value of $f = 10.8\%$ was observed. Note that in this case, despite the structural disorder, torsional order is imparted to the P3HT. On the basis of these results, for a single P3HT 20-mer at the interface with SWNTs an increase in conjugation length by a factor of f_{300}/f in the range 2−25 is found compared to that for an isolated P3HT chain.

These results indicate that the inherent 1-dimensional (1D), cylindrical shape of the SWNTs limits the torsional disorder of P3HT upon adsorption and acts as a template to impart a longer polymer conjugation length. Single frames with helical conformations (Figure 2a) are found to have $f = 0$, which confirms that torsional order is imparted to the adsorbed P3HT by $\pi-\pi$ coplanar stacking of P3HT and SWNTs.

Once again, to explore this effect unbiased by the initial P3HT configuration we performed the same analysis on the larger simulation runs with different SWNT concentrations and lengths described above. To obtain these data, we averaged the f values found in separate, uncorrelated frames sampled every 100 ps in the second half of the simulation run ($t > 500$ ps, when P3HT adsorption is practically complete, as shown in Figure 3), for a total of 8−10 frames. Since a large number of chains is used, the standard deviation of f reduces to $\sigma_f \approx 0.01$ (or 1%), and the collected data is representative of the average conjugation length. The full analysis for all the cases explored is reported in Figure 5.

At 0% SWNT concentration (*i.e.,* for pure P3HT in the form of 20-mer chains at 1/40 the condensed phase density) a value of $f = 26.5\%$ is found, in close agreement with the single chain case. This means that P3HT−P3HT interactions do not soften significantly the torsional degrees of freedom of the chains. As the concentration of SWNTs increases, the fraction f decreases monotonically, and the conjugation length $1/f$ increases accordingly. For example, for 15 nm long SWNTs (*i.e.*, almost as long as the simulation cell side) the conjugation length increases from approximately 1/0.25 = 4 rings for pure P3HT to 1/0.1 = 10 rings (approximately 5 nm) for a concentration of 40% by weight (or about 20% by volume) of SWNTs. Note that the lower limit attained at high concentration is close to the upper limit of $f = 10.8\%$ for a single P3HT molecule at the interface with P3HT, which in fact corresponds to a very high SWNT concentration. The rate at which $1/f$ increases is higher for the 15 nm long nanotubes than for the 5 nm long nanotubes due to their higher

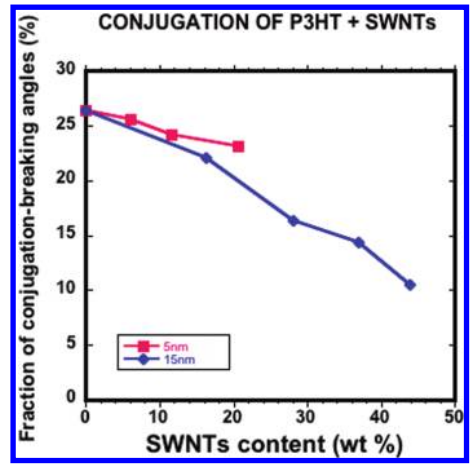

Figure 5. Fraction of conjugation-breaking angles f for different SWNT concentration in P3HT−SWNT simulation runs with varying SWNT concentrations and lengths. The conjugation length $1/f$ increases monotonically as the SWNT concentration is increased, at a higher rate for longer SWNTs due to the higher SWNT aspect ratio. These results show that torsional order and increased conjugation length are imparted by the SWNTs to the conjugated P3HT polymer.

aspect ratio which favors P3HT adsorption on the sidewalls. This suggests that the key role in imparting the torsional order is played by the SWNT sidewalls and specifically by the coplanar $\pi-\pi$ stacking as observed above. Experimental results seem to confirm these trends. Raman measurements recently performed by Giulianini *et al.*[16] revealed a 6 cm^{-1} downshift of the P3HT $C_\alpha{=}C_\beta$ stretching vibration in multiwalled nanotubes (MWNTs)−P3HT composites that was previously attributed to increased P3HT conjugation length. To further investigate this point, we carried out measurements of the optical absorption spectra of double-walled nanotubes (DWNTs)−P3HT thin film composites at different DWNT concentrations, prepared by spin-casting (see Supporting Information for details). In these experiments, the use of DWNTs is preferred to SWNTs due to their superior transparency in the visible,[36] mechanical stiffness, and thermal stability,[37] while the templating effect and the interface self-assembly should be unaltered due to the closely related structures. Our results for the measured absorption spectrum are shown in Figure 6a.

The $\pi-\pi^*$ transitions are found at 566 nm (2.19 eV) and 512 nm (2.42 eV, peak with maximum intensity). These are due, respectively, to the 0−0 and the 0−1 transitions, where 0−n means a vibronic transition from the ground vibrational state of the ground singlet electronic state to the nth vibrational state of the first excited singlet electronic state, and are in very good agreement with values reported in the literature.[38]

The shoulder at 615 nm (2.02 eV) represents a transition of a different nature. Brown *et al.*[38] showed compelling evidence that this transition can be attributed to an interchain absorption, corresponding to the formation of an exciton delocalized over multiple P3HT

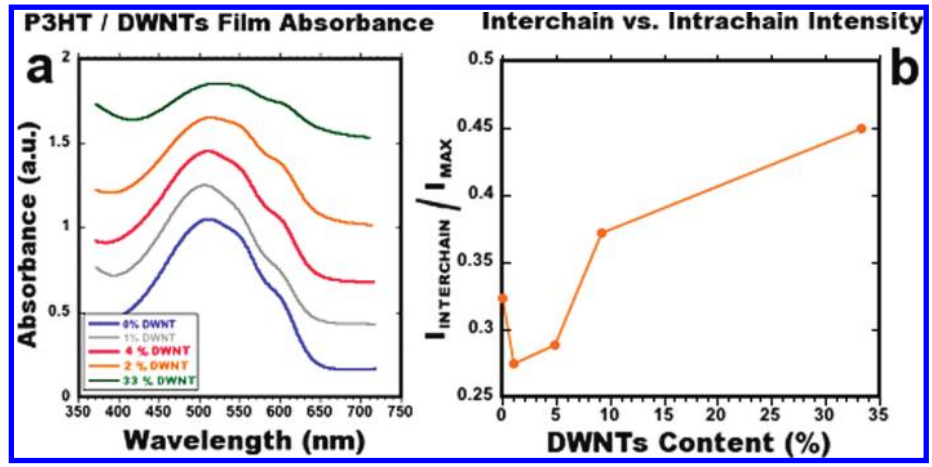

Figure 6. (a) Absorption spectrum (arbitrary units) of P3HT−DWNT composites at different weight fractions. The curves are shifted to different baseline height for clarity. As the concentration increases, the overall intensity decreases due to the presence of less P3HT in the composite. (b) An increase in the ratio of the intensity of the peak at 615 nm *vs* the intensity of the maximum at higher DWNT concentrations is attributed to increased conjugation order in the system, as seen in the MD simulations.

chains, the intensity of which is correlated to the degree of (torsional) order in the polymer.

As the DWNT concentration is increased from 0 to 33% wt, we observed an increase in the relative intensity of the interchain transition at 615 nm compared to the maximum (0−1) intensity (Figure 6b), by a factor of 1.45 for the highest DWNT concentration.[39] This can be understood from the fact that when torsional rotations of the thiophene rings are reduced due to the ordering effect from SWNTs (or DWNTs), the overlap of the wave functions of neighboring chains increases and so does the magnitude of interchain coupling[38] and therefore the intensity of the interchain absorption.

A slight red-shift (<5 nm) of all the peaks is also observed in the presence of DWNTs likely due to charge transfer between the P3HT and the DWNTs. We found analogous results for blends of MWNTs and P3HT (see Supporting Information). These experimental results, together with the MD simulations, provide strong evidence for favorable increase in the system π-conjugation due to interface effects upon carbon nanotubes mixing with P3HT.

It is interesting to note that in current P3HT−SWNT devices a maximum concentration of approximately 3−5% wt SWNTs is used to avoid short-circuiting[5] from the metallic SWNTs and to allow for extensive absorption from the polymer layer. Conversely, our results show that (apart from practical limitations) a better regime to prepare SWNT−P3HT photovoltaic devices might be the use of a much higher fraction of SWNTs to take advantage of the SWNTs templating effect that enhances the polymer conjugation and consequently the charge transfer. The SWNTs should be properly debundled and of semiconductive type, both for the favorable electronic structure[4] and to avoid short-circuiting.[5]

Impact of Self-Assembly on the Interface Charge Transfer. To assess the impact of the P3HT conjugation length on the charge transfer, a simple model for a rate of tunneling varying as e^{-kd} (d = distance of localized electronic state on the P3HT chain to the SWNT surface, k = constant depending on the model used to describe tunneling) allows one to understand that torsional order imparted by cofacial π−π stacking causes on average a smaller separation and greater overlap between the polymer and the SWNT electronic states. If an electron transitions nonadiabatically and elastically from the P3HT conduction band to the SWNT conduction band (assumed as a large reservoir of electronic states), a larger conjugation in the P3HT electronic states would favor the charge transfer. For two polymers of different conjugation lengths (one of longer conjugation length $L_> = 1/f_>$ and one of shorter conjugation length $L_< = 1/f_<$) an increase in the charge transfer rate due to the increased conjugation length can be estimated using Bardeen's tunneling theory[40] to be on the order of at least $O(L_>/L_<)$ (see the Supporting Information for a full derivation).[41] Therefore, for a doubling of the conjugation length (with respect to a blend with 2% wt SWNTs), achievable using approximately 30% wt SWNTs according to Figure 5, an increase in the charge transfer rate by a factor of 2−20 could be observed. This is clearly only a rough estimate of how the interface structure could affect the charge transfer in the P3HT−SWNT system; whether or not this mechanism is the dominant one in determining the charge transfer rate at this interface remains largely an open question.[43,44]

CONCLUSION

We have investigated the self-assembly of P3HT and SWNTs using MD simulations and showed that it is guided by π−π stacking interactions and occurs rapidly (100 ps) leading to irreversible P3HT adsorption. Our MD simulations reveal many of the conformations observed in recent experiments, including helices, bundles, and more elongated conformations that

maximize planar $\pi-\pi$ stacking. From an analysis of the π-conjugation we showed that SWNTs, due to their intrinsic 1D, cylindrical shape and π-conjugation, impart a longer conjugation length to P3HT chains adsorbed at their surface by quenching their torsional disorder, regardless of their conformation and nanotube chirality. The effect is more significant for higher SWNT weight fractions in the sample (since this is an interface effect) and could favor charge transfer in type-II forming all-semiconducting SWNT−P3HT blends prepared with a higher SWNT content. We suggest that the P3HT interface ordering and consequent charge transfer enhancement could be present in a larger number of polymer donor and 1D acceptor systems, that would thus perform better when a higher weight fraction of the 1D inorganic material is used. With recent advances in carbon nanotube sorting and selective synthesis[14] and in nanoscale characterization of bulk heterojunctions,[42] mixtures of all-semiconducting SWNTs and P3HT (or similar conjugated polymers) could continue to push the existing barriers in the use of carbon nanotubes in XSC.

METHODS

Molecular Dynamics Simulations. We used the force field from Marcon *et al.*[24] to model the P3HT molecules, both for the intramolecular and the intermolecular P3HT−P3HT interaction terms. This provides a balanced description of the intramolecular degrees of freedom which are mostly derived from the MM3 parametrization[25] and uses an accurate inter-ring torsion potential based on *ab initio* calculations (MP2/aug-cc-pVTZ) of 2,2′-bithiophene.[24] Potential-derived charges are placed on all atoms and were obtained from gas-phase B3LYP/6-31G calculations on tetra-thiophene.[24] The AMBER99 force field[26] was used to model the interaction between the SWNT and the P3HT molecule;[27] on the basis of previous work,[20,28] the SWNT atoms were modeled as uncharged Lennard-Jones particles using sp^2 carbon parameters from the AMBER99 force field. All cutoffs of nonbonded terms were set to 12 Å. The $\pi-\pi$ stacking interaction plays a critical role in the self-assembly of SWNTs with P3HT due to the delocalized nature of electronic states deriving from mixtures of carbon p_z orbitals in both species. In the AMBER99 force field, stacking interactions among aromatic species are parametrized within the van der Waals parameters of each atom type. Specific electrostatic interactions among π electrons are thus included in an average way, but the overall framework has proven reliable to study $\pi-\pi$ stacking forces.[20] The SWNT intramolecular degrees of freedom were initially modeled using the Tersoff potential for carbon,[29,30] although freezing the SWNTs in the simulation led to identical self-assembly and dynamics of the polymer; thus, in most simulations the SWNTs were modeled as rigid bodies interacting with P3HT through van der Waals forces. This means that the energy scale of the SWNT vibrations is much smaller than that involved in the P3HT dynamics at the interface for the temperatures considered. The simulation runs consisted of 100 ps equilibration followed by 0.5−1.5 ns production time. Additional computational details are provided in the Supporting Information.

Supporting Information Available: Details of the MD simulations and computational procedures; videos of a number of simulation runs of P3HT and SWNTs; preparation and experimental setup for the optical absorption measurements; additional optical spectra; discussion and estimate of the impact of the conjugation length on the interface charge transfer. This material is available free of charge *via* the Internet at http://pubs.acs.org.

REFERENCES AND NOTES

1. Zhu, H.; Wei, J.; Wang, K.; Wu, D. Applications of Carbon Materials in Photovoltaic Solar Cells. *Sol. Energy Mater. Sol. Cells* **2009**, *93*, 1461–1470.
2. Mayer, A. C.; Scully, S. R.; Hardin, B. E.; Rowell, M. W.; McGehee, M. D. Polymer-Based Solar Cells. *Mater. Today* **2007**, *10*, 28–33.
3. Kymakis, E.; Amaratunga, G. A. J. Single-Wall Carbon Nanotube/Conjugated Polymer Photovoltaic Devices. *Appl. Phys. Lett.* **2002**, *80*, 112–114.
4. Kanai, Y.; Grossman, J. C. Role of Semiconducting and Metallic Tubes in P3HT/Carbon-Nanotube Photovoltaic Heterojunctions: Density Functional Theory Calculations. *Nano Lett.* **2008**, *8*, 908–912.
5. Kymakis, E.; Amaratunga, G. A. J. Solar Cells Based on Composites of Donor Conjugated Polymers and Carbon Nanotubes. *Organic Photovoltaics*; Sun, S.-S., Sariciftci, N. S., Eds.; CRC Press: Boca Raton, FL, 2005.
6. Kymakis, E. The Impact of Carbon Nanotubes on Solar Energy Conversion. *Nanotechnol. Law Bus.* **2006**, *3*, 405–410.
7. Li, C.; Chen, Y.; Wang, Y.; Iqbal, Z.; Chhowalla, M.; Mitra, S. A Fullerene-Single Wall Carbon Nanotube Complex for Polymer Bulk Heterojunction Photovoltaic Cells. *J. Mater. Chem.* **2007**, *17*, 2406–2411.
8. Ma, W.; Yang, C.; Gong, X.; Lee, K.; Heeger, A. Thermally Stable, Efficient Polymer Solar Cells with Nanoscale Control of the Interpenetrating Network Morphology. *J. Adv. Funct. Mater.* **2005**, *15*, 1617–1622.
9. Kymakis, E.; Amaratunga, G. A. J. Optical Properties of Polymer−Nanotube Composites. *Synth. Met.* **2004**, *142*, 161–167.
10. Kymakis, E.; Alexandrou, I.; Amaratunga, G. A. J. Single-Walled Carbon Nanotube−Polymer Composites: Electrical, Optical, and Structural Investigation. *Synth. Met.* **2002**, *127*, 59–62.
11. Chen, L.-M.; Hong, Z.; Li, G.; Yang, Y. Recent Progress in Polymer Solar Cells: Manipulation of Polymer:Fullerene Morphology and the Formation of Efficient Inverted Polymer Solar Cells. *Adv. Mater.* **2009**, *21*, 1434–1449.
12. Yang, C.; Hu, J. G.; Heeger, A. J. Molecular Structure and Dynamics at the Interface within Bulk Heterojunction Materials for Solar Cells. *J. Am. Chem. Soc.* **2006**, *128*, 12007–12013.
13. Hersam, M. C. Progress Towards Monodisperse Single-Walled Carbon Nanotubes. *Nat. Nanotechnol.* **2008**, *3*, 387–394.
14. Liu, J.; Hersam, M. C. Recent Developments in Carbon Nanotube Sorting and Selective Growth. *MRS Bull.* **2010**, *35*, 315–321.
15. Giulianini, M.; Waclawick, E.; Bell, J. M.; De Crescenzi, M.; Castrucci, P.; Scarselli, M.; Motta, N. Regioregular Poly(3-hexyl-thiophene) Helical Self-Organization on Carbon Nanotubes. *Appl. Phys. Lett.* **2009**, *95*, 013304.
16. Giulianini, M.; Waclawik, E.; Bell, J. M.; Scarselli, M.; Castrucci, P.; De Crescenzi, M.; Motta, N. Evidence of Multiwall Carbon Nanotube Compression Caused by Poly(3-hexylthiophene) Adhesion. Submitted for publication.
17. Gu, H.; Swager, T. M. Fabrication of Free-Standing, Conductive, and Transparent Carbon Nanotube Films. *Adv. Mater.* **2008**, *20*, 4433–4437.
18. Jensen, F. *Introduction to Computational Chemistry*, 2nd ed.; John Wiley & Sons: Chichester, England, 2007.
19. Frenkel, D.; Smit, B. *Understanding Molecular Simulation*, 2nd ed.; Academic Press: Bodmin, Great Britain, 2002.
20. Johnson, R. R.; Johnson, A. T. C.; Klein, M. L. Probing the Structure of DNA−Carbon Nanotube Hybrids with Molecular Dynamics. *Nano Lett.* **2008**, *8*, 69–75.

21. Vukmirovic, N.; Wang, L.-W. Electronic Structure of Disordered Conjugated Polymers: Polythiophenes. *J. Phys. Chem. B* **2009**, *113*, 409–415.
22. LAMMPS Molecular Dynamics Simulator. http://lammps.sandia.gov. (Accessed March 1, 2010).
23. Plimpton, S. J. Fast Parallel Algorithms for Short-Range Molecular Dynamics. *J. Comput. Phys.* **1995**, *117*, 1–19.
24. Marcon, V.; Raos, G. Molecular Modeling of Crystalline Oligothiophenes: Testing and Development of Improved Force Fields. *J. Phys. Chem. B* **2004**, *108*, 18053–18064.
25. Allinger, N. L.; Yuh, Y. H.; Lii, J.-H. Molecular Mechanics. The MM3 Force Field for Hydrocarbons. 1. *J. Am. Chem. Soc.* **1989**, *111*, 8551.
26. Cornell, W. D.; Cieplak, P.; Bayly, C. I.; Gould, I. R.; Merz, K. M.; Ferguson, D. M.; Spellmeyer, D. C.; Fox, T.; Caldwell, J. W.; Kollman, P. A. A Second Generation Force Field for the Simulation of Proteins, Nucleic Acids, and Organic Molecules. *J. Am. Chem. Soc.* **1995**, *117*, 5179–5197.
27. MM3 intramolecular interactions complete the description of the inter-ring torsional barriers and therefore must be used to model the P3HT intramolecular and P3HT-P3HT intermolecular non-bonded terms. On the other hand, the AMBER force field has been tested more extensively to account for the interaction of molecules with SWNTs (see ref. 20) and thus this parametrization was chosen to describe the P3HT−SWNT intermolecular interaction.
28. Hummer, G.; Rasaiah, C.; Noworyta, J. P. Water Conduction through the Hydrophobic Channel of a Carbon Nanotube. *Nature* **2001**, *414*, 188–190.
29. Tersoff, J. New Empirical Approach for the Structure and Energy of Covalent Systems. *Phys. Rev. B* **1988**, *37*, 6991–7000.
30. Tersoff, J. Modeling Solid-State Chemistry: Interatomic Potentials for Multicomponent Systems. *Phys. Rev. B* **1989**, *39*, 5566–5568.
31. Note that our calculations do not contain explicit solvent molecules; however, the most significant effect from a *non-polar* solvent may be a slight screening of the charges within a same P3HT chain. A *non-polar* solvent such as chloroform or toluene, commonly used in P3HT−SWNT solutions for solar cell preparation, would interact in a comparable manner with P3HT and SWNTs, with a net effect (to a first approximation) of slowing down the dynamics of the system without modifying the self-assembly significantly. Introduction of a *polar* solvent (like water) would instead change the self-assembly dramatically and lead to significant aggregation within the hydrophobic SWNT and P3HT phases, but for this reason this is not used in practical circumstances for preparation of bulk-heterojunction solar cells. Thus our results refer to the self-assembly in a *non-polar* solvent.
32. In Figure 3, PBC have been unwrapped for ease of visualization. This means that all-P3HT domains exist but cannot be seen due to the unwrapping, that causes molecules to move to adjacent cells instead of re-entering the same simulation cell. Clearly all-P3HT domains far from the interface do not crystallize during the simulation as occurs in reality, as this is an intrinsic limit of MD simulations. This does not limit the possibility of studying the very first few layers adjacent to the SWNT−P3HT interface, where crystalline order is in any case disrupted by the SWNTs presence.
33. Bredas, J. L.; Street, G. B.; Themans, B.; Andre, J. M. Organic Polymers Based on Aromatic Rings (Polyparaphenylene, Polypirrole, Polythiophene): Evolution of the Electronic Properties as a Function of the Torsion Angle between Adjacent Rings. *J. Chem. Phys.* **1985**, *83*, 1323–1329.
34. To allow for a 5% tolerance, we actually chose 42° as the threshold value for an angle to be defined as "conjugation-breaking". We calculated *f* every ps in a 1 ns run, discarded the first 100 ps (equilibration), and averaged to obtain the final *f* value.
35. Note that while the standard deviation can be significant for a single P3HT chain with 40 rings where the number of sampled ring−ring torsion angles is only 38, when a large number of chains is present in the simulation run the standard deviation decreases significantly (and would go to zero in the limit of infinitely long chains).
36. Wei, J. Q.; Jia, Y.; Shu, Q. K.; Gu, Z. Y.; Wang, K. L.; Zhuang, D. M.; Zhang, G.; Wang, Z. C.; Luo, J. B.; Cao, A. Y.; Wu, D. H. Double-Walled Carbon Nanotube Solar Cells. *Nano Lett.* **2007**, *7*, 2317–2321.
37. Endo, M.; Muramatsu, H.; Hayashi, T.; Kim, Y. A.; Terrones, M.; Dresselhaus, M. S. 'Buckypaper' from Coaxial Nanotubes. *Nature* **2005**, *433*, 476.
38. Brown, P. J.; Thomas, D. S.; Kohler, A.; Wilson, J. S.; Kim, J.-S.; Ramsdale, C. M.; Sirringhaus, H.; Friend, R. H. Effect of Interchain Interactions on the Absorption and Emission of Poly(3-hexylthiophene). *Phys. Rev. B* **2003**, *67*, 064203.
39. The relatively slight increase is consistent with the fact that this is mostly an interface effect. Since even at the highest DWNT concentrations the volume fraction of the P3HT is around 80−90%, a relatively small effect has to be expected. The points at small DWNT concentrations below 5% should therefore be considered as a single value despite fluctuations of about 10% in the intensity ratio. This sets the accuracy for these estimates with our method. On the other hand, the increase in the intensity ratio at higher DWNT concentrations is significant and consistent with the other evidences and with the spectra for MWNT−P3HT in the Supporting Information.
40. Bardeen, J. Tunneling from a Many-Particle Point of View. *Phys. Rev. Lett.* **1961**, *6*, 57–59.
41. Note that the same ordering effect is essentially responsible for more efficient charge transfer in crystalline P3HT regions compared to disordered P3HT regions. For example, see: Salleo, A. Charge Transport in Polymeric Transistors. *Mater. Today* **2007**, *10*, 38. The description is analogous here since the interchain transport in the $\pi-\pi$ interchain stacking crystalline direction can be described as a tunneling event. Additionally, the exciton binding energy should decrease as the conjugation length increases, thus facilitating electron-hole separation within the P3HT and electron injection into the SWNT phase.
42. Hamadani, B. H.; Jung, S.; Haney, P. M.; Richter, L. J.; Richter, L. J.; Zhitenev, N. B. Origin of Nanoscale Variations in Photoresponse of an Organic Solar Cell. *Nano Lett.* **2010**, *10*, 1611–1617.
43. For a more complete assessment of charge transfer at this interface, several other mechanisms and factors should be considered: the presence of Forster resonant energy transfer, the existence of a charge transfer state, the possibility of non-adiabatic (*vs* adiabatic) charge transfer as assumed here, and a correct level alignment (in an independent electron picture of the interface) at the P3HT−SWNT interface, which is partially explored in ref 4 but is still largely an open problem. The application of more accurate approaches than DFT, which is beyond the scope of this investigation, would also be of great value in an attempt to gain insight into the charge transfer mechanism (see, *e.g.*, ref 44).
44. Kanai, Y.; Wu, Z.; Grossman, J. C. Charge Separation in Nanoscale Photovoltaic Materials: Recent Insight from First-Principle Electronic Structure Theory. *J. Mater. Chem.* **2010**, *20*, 1053–1061.